# Study of $\chi_{cJ}$ (J = 0,1,2) decays to light meson pairs based on SU(3) flavor symmetry/breaking analysis\*

Bo Lan (兰波)<sup>1</sup> Qin-Ze Song (宋沁泽)<sup>1</sup> Jin-Huan Sheng (盛金环)<sup>2</sup> Yi Qiao (乔怡)<sup>3</sup> Ru-Min Wang (王茹敏)<sup>1†</sup>

<sup>1</sup>College of Physics and Communication Electronics, Jiangxi Normal University, Nanchang 330022, China <sup>2</sup>School of Physics and Engineering, Henan University of Science and Technology, Luoyang 471000, China <sup>3</sup>College of Physics and Electronic Information, Nanchang Normal University, Nanchang 330032, China

**Abstract:** Based on available experimental results on  $\chi_{cJ}(J=0,1,2)$  decays, we investigated the  $\chi_{cJ} \to PP$ , VV, PV, and PT decays using the SU(3) flavor symmetry/breaking approach, where P, V, and T denote light pseudoscalar, vector, and tensor mesons, respectively. With the decay amplitude relations determined by SU(3) flavor symmetry/breaking, we present the branching ratios for all  $\chi_{cJ} \to PP$  and  $\chi_{cJ} \to VV$  modes, including those without experimental data. While theoretical considerations strongly suppress or even forbid most  $\chi_{cJ} \to PV$  and PT decays, we also provide quantitative predictions constrained by existing experimental data. Our results are expected to be accessible in future experiments at BESIII and the planned Super Tau-Charm Facility.

Keywords: charmonium decays, SU(3) symmetry/breaking, light meson pairs

**DOI:** 10.1088/1674-1137/adff00 **CSTR:** 32044.14.ChinesePhysicsC.49123106

#### I. INTRODUCTION

The triplet state  $\chi_{cJ}(J=0,1,2)$ , as the lowest energy P-wave charmonium, has not been widely studied in the past because it cannot be directly obtained from  $e^+e^-$  collisions. However,  $\psi(3686)$  provides a clean environment for the production of  $\chi_{cJ}$  mesons via electromagnetic decays such as  $\psi(3686) \rightarrow \gamma \chi_{cJ}$ . Given that  $\psi(3686)$  has been widely studied and measured [1–5], more and better measurements of  $\chi_{cJ}$  decays have been collected, leading to increased interest in the study of hadronic decays of the  $\chi_{cJ}$  states [6–12].

Hadronic  $\chi_{cJ}$  decays have great significance for studying strong force dynamics. On the one hand, the scale of charm quark mass (~1.5 GeV) lies between perturbative and non-perturbative QCD in theoretical calculations; it is neither large enough for significant heavy quark expansion nor small enough for perturbation theory [13, 14]. On the other hand, most of the hadronic  $\chi_{cJ}$  decays are suppressed by the Okubo-Zweig-Iizuka (OZI) rule [15]. Moreover, there are still theoretical and experimental discussions regarding the doubly OZI-suppressed and singly OZI-suppressed decay mechanisms in some processes [16–20]. Owing to these characteristics, understanding hadronic  $\chi_{cJ}$  decay mechanisms is important for

improving theoretical models of both perturbative and non-perturbative QCD. These mechanisms offer a valuable framework for testing phenomenological models and constraining theoretical parameters.

The  $\chi_{cJ}$  mesons that decay into the two-meson states are particularly useful and they are relatively straightforward to detect and model theoretically. One important feature of charmonium hadronic decays into light mesons is that they are processes rich in gluons. The initial c and  $\bar{c}$  quarks annihilate into gluons, which then hadronize to produce the final state of light quarks [21]. Furthermore, the quantum numbers  $(I^G J^{PC})$  of mesons produced by two photons that decay into PP, VV are restricted; they must be 0+ for isospin and even++ for parity and charge conjugation; this is the case of  $\chi_{cJ}(J = even)$  mesons. Specifically, owing to spin parity conservation,  $\chi_{c1}$  cannot decay into two pseudoscalar mesons. Moreover, they violate the so-called helicity selection rule, which is defined as  $\sigma = (-1)^J P$  [22] and requires  $\sigma^{\text{initial}} = \sigma_1 \sigma_2$ , where J and P are respectively the spin and parity of the particle.

The theoretical calculations of charmonium decays have always been notably difficult. The non-relativistic QCD (NRQCD) framework [23, 24] and phenomenological approaches are suitable and effective to study the charmonium decays. Previous studies of hadronic  $\chi_{cJ}$  de-

Received 10 June 2025; Accepted 24 August 2025; Published online 25 August 2025

<sup>\*</sup> Supported by the National Natural Science Foundation of China (12175088, 12305100, 12365014) and Graduate Innovation Fund Project of Jiangxi Provincial Department of Education (YJS2024091)

<sup>†</sup> E-mail: ruminwang@sina.com

Content from this work may be used under the terms of the Creative Commons Attribution 3.0 licence. Any further distribution of this work must maintain attribution to the author(s) and the title of the work, journal citation and DOI. Article funded by SCOAP<sup>3</sup> and published under licence by Chinese Physical Society and the Institute of High Energy Physics of the Chinese Academy of Sciences and the Institute of Modern Physics of the Chinese Academy of Sciences and IOP Publishing Ltd

cays used various theoretical frameworks, including parametrization schemes [16, 25], intermediate hadronic loops [18, 26], quark pair creation model with perturbative QCD (pQCD) framework [27], and a description within the effective field theory framework [28]. In Refs. [16, 25], parametrization schemes were proposed to further understand the mechanism of violating OZI rules in the two body decays of  $\chi_{cJ} \rightarrow PP, VV, SS$ , where S denotes scalar meson. These studies suggest that, in addition to singly OZI-suppressed processes, doubly OZI-suppressed processes may play a significant role in the production of isospin-0 light meson pairs, such as  $\chi_{c1} \rightarrow f_0f_0'$ ,  $\omega\omega$ ,  $\phi\phi$ ,  $\omega\phi$ ,  $\eta\eta$ ,  $\eta\eta'$ , and  $\eta'\eta'$ .

In this study, we perform a SU(3) flavor symmetry and breaking analysis of charmonium decay processes  $\chi_{cJ} \rightarrow PP$ , VV, PV, and PT. In Sec. II, the fundamental amplitude relations and theoretical frameworks governing the  $\chi_{cJ} \rightarrow PP$ , VV decays are described. Subsequently, numerical results related to  $\chi_{cJ} \rightarrow PP$ , VV decays obtained from present experimental data are reported. In Sec. III, corresponding amplitude relations and numerical results of the  $\chi_{cJ} \rightarrow PV$ , PT decays are presented. Final conclusions are provided in Sec. IV.

## **II.** $\chi_{cJ} \rightarrow PP, VV$ **DECAYS**

#### A. Amplitude Relations of $\chi_{cJ} \rightarrow PP, VV$

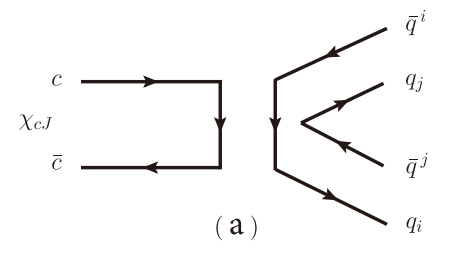
The pseudoscalar and vector meson octet states under SU(3) flavor symmetry of u,d,s quarks can be expressed as

$$P = \begin{pmatrix} \frac{\pi^{0}}{\sqrt{2}} + \frac{\eta_{8}}{\sqrt{6}} + \frac{\eta_{1}}{\sqrt{3}} & \pi^{+} & K^{+} \\ \pi^{-} & -\frac{\pi^{0}}{\sqrt{2}} + \frac{\eta_{8}}{\sqrt{6}} + \frac{\eta_{1}}{\sqrt{3}} & K^{0} \\ K^{-} & \bar{K}^{0} & -\frac{2\eta_{8}}{\sqrt{6}} + \frac{\eta_{1}}{\sqrt{3}} \end{pmatrix},$$

$$(1)$$

and

$$V = \begin{pmatrix} \frac{\rho^0}{\sqrt{2}} + \frac{\omega_8}{\sqrt{6}} + \frac{\omega_1}{\sqrt{3}} & \rho^+ & K^{*+} \\ \rho^- & -\frac{\rho^0}{\sqrt{2}} + \frac{\omega_8}{\sqrt{6}} + \frac{\omega_1}{\sqrt{3}} & K^{*0} \\ K^{*-} & \bar{K}^{*0} & -\frac{2\omega_8}{\sqrt{6}} + \frac{\omega_1}{\sqrt{3}} \end{pmatrix},$$
(2)



where  $\eta_1$ - $\eta_8$  and  $\omega_1$ - $\omega_8$  denote unmixed states; according to Particle Data Group (PDG) [29], the mixings of  $\eta$ - $\eta'$  and  $\phi$ - $\omega$  are described as follows:

$$\eta = (\eta_8 \cos \theta_P - \eta_1 \sin \theta_P), \tag{3}$$

$$\eta' = (\eta_8 \sin \theta_P + \eta_1 \cos \theta_P), \tag{4}$$

and

$$\phi = (\omega_8 \cos \theta_V - \omega_1 \sin \theta_V), \tag{5}$$

$$\omega = (\omega_8 \sin \theta_V + \omega_1 \cos \theta_V). \tag{6}$$

Many previous theoretical studies considered the mesons  $\omega$  and  $\eta$  as pure octet components. Experimental observations showed that  $\omega$  and  $\eta$  are mixtures of both octet and singlet components, with a specific mixing angle. Therefore, we discuss the branching ratio results that incorporate the  $\eta$ - $\eta'$  and  $\phi$ - $\omega$  mixings with mixing angle values from PDG, with  $\theta_P = [-20^\circ, -10^\circ]$  and  $\theta_V = 36.5^\circ$  [29].

As shown in Fig. 1, the singly OZI and doubly OZI disconnected decay modes are considered. Fig. 1(a) shows a typical singly OZI process, where gluons produced by initial state annihilation create new quark pairs and undergo quark exchange in the final state. In Fig. 1(b), two quark pairs are created by gluons and recoil without quark exchanges, which show a doubly OZI process. Based on SU(3) flavor symmetry, the decay amplitudes of the decay  $\chi_{cJ} \rightarrow MM$  can be parametrized as

$$\mathcal{A}^{s}(\chi_{cJ} \to M_{1}M_{2}) = a^{M}_{1J}M^{i}_{1j}M^{j}_{2i} + a^{M}_{2J}M^{i}_{1i}M^{j}_{2j}, \qquad (7)$$

where M = P/V, i, j = 1, 2, 3 correspond to the matrix elements in Eqs. (1)–(2);  $a_{1J}^M$  and  $a_{2J}^M$  are non-perturbative coefficients corresponding to the decay modes in Figs. 1(a) and (b), respectively. The specific decay amplitudes for  $\chi_{cJ} \rightarrow PP, VV$  with SU(3) flavor symmetry are listed in the second column of Table 1.

The SU(3) flavor symmetry assumes that u, d, and s quarks have equal masses. SU(3) flavor symmetry breaking is given by the current quark mass term in the QCD Lagrangian with  $m_{u,d} \ll m_s$  in the Standard Model. To

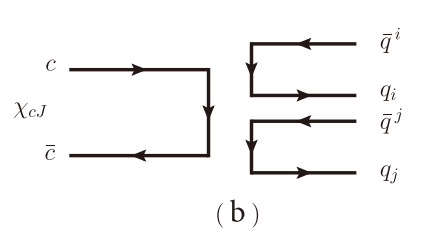


**Fig. 1.** Singly OZI disconnected (a) and doubly OZI disconnected (b) diagrams of  $\chi_{cJ} \rightarrow MM$  decays.

| Decay modes                                              | Symmetry amplitudes                                                      | Breaking amplitudes                                          |
|----------------------------------------------------------|--------------------------------------------------------------------------|--------------------------------------------------------------|
| $\chi_{cJ} \to \pi^+ \pi^- / \rho^+ \rho^-$              | $2a_{1J}^M$                                                              | $2b_J^M$                                                     |
| $\chi_{cJ} \rightarrow K^+K^-/K^{*+}K^{*-}$              | $2a_{1J}^M$                                                              | $-b_J^M$                                                     |
| $\chi_{cJ} \to K^0 \bar{K}^0 / K^{*0} \bar{K}^{*0}$      | $2a_{1J}^M$                                                              | $-b_J^M$                                                     |
| $\chi_{cJ}  ightarrow \pi^0 \pi^0 /  ho^0  ho^0$         | $\sqrt{2}a_{1J}^{M}$                                                     | $\sqrt{2}b_J^M$                                              |
| $\chi_{cJ}  ightarrow \eta_1 \eta_1/\omega_1 \omega_1$   | $\sqrt{2}(a_{1J}^M + 3a_{2J}^M)$                                         | 0                                                            |
| $\chi_{cJ}  ightarrow \eta_1 \eta_8/\omega_1 \omega_8$   | 0                                                                        | $2\sqrt{2}b_J^M$                                             |
| $\chi_{cJ}  ightarrow \eta_8 \eta_8 / \omega_8 \omega_8$ | $\sqrt{2}a_{1J}^{M}$                                                     | $-\sqrt{2}b_J^M$                                             |
| $\chi_{cJ} 	o \eta \eta/\phi \phi$                       | $\sqrt{2}a_{1J}^M + \frac{3\sqrt{2}}{2}a_{2J}^M(1-\cos 2\theta_M)$       | $-\sqrt{2}b_J^M\cos\theta_M(4\sin\theta_M+\cos\theta_M)$     |
| $\chi_{cJ} 	o \eta \eta'/\phi \omega$                    | $-\frac{3\sqrt{2}}{2}a_{2J}^M\sin2\theta_M$                              | $\sqrt{2}b_J^M(2\cos 2\theta_M - \frac{1}{2}\sin 2\theta_M)$ |
| $\chi_{cJ} 	o \eta' \eta' / \omega \omega$               | $\sqrt{2}a_{1J}^{M} + \frac{3\sqrt{2}}{2}a_{2J}^{M}(1+\cos 2\theta_{M})$ | $\sqrt{2}b_J^M\sin\theta_M(4\cos\theta_M-\sin\theta_M)$      |

**Table 1.** SU(3) symmetry and breaking amplitudes of  $\chi_{cJ} \to P_1 P_2$  and  $\chi_{cJ} \to V_1 V_2$ .

conduct a more accurate analysis, we take into account the symmetry breaking. The diagonalized mass matrix can be expressed as [30-32]

$$\begin{pmatrix} m_u & 0 & 0 \\ 0 & m_d & 0 \\ 0 & 0 & m_s \end{pmatrix} = \frac{1}{3}(m_u + m_d + m_s)I + \frac{1}{2}(m_u - m_d)X + \frac{1}{6}(m_u + m_d - 2m_s)W,$$
(8)

where I is the identity matrix, and X and W are represented as

$$X = \begin{pmatrix} 1 & 0 & 0 \\ 0 & -1 & 0 \\ 0 & 0 & 0 \end{pmatrix}, \quad W = \begin{pmatrix} 1 & 0 & 0 \\ 0 & 1 & 0 \\ 0 & 0 & -2 \end{pmatrix}. \quad (9)$$

Considering the mass difference between the s quark and the u, d quarks, the W part of the diagonalized mass matrix is included to account for symmetry breaking. Thus, the amplitude of the breaking part can be written as

$$\mathcal{A}^b(\chi_{cJ} \to M_1 M_2) = b_J^M M_{1j}^i W_k^j M_{2i}^k,$$
 (10)

where  $b_J^M$  is the non-perturbative coefficient of the breaking term. The decay amplitudes for  $\chi_{cJ} \rightarrow P_1 P_2, V_1 V_2$  with SU(3) breaking are listed in the third column of Table 1. Note that the minus signs of the breaking terms arise from the mathematical structure of the W matrix given in Eq. (9). Furthermore, we follow a similar convention to that of Refs. [33, 34], regarding the final state being identical particles, where the amplitude of the final state

of identical particles is multiplied by a coefficient with  $\sqrt{2}$ .

In general, the three parameters involved  $(a_{1J}^M, a_{2J}^M, b_J^M)$  are complex. Given that an overall phase can be removed without losing generality, we set  $a_{1J}^M$  to be real. Five real independent parameters are considered in data analysis:

$$a_{1J}^M$$
,  $a_{2J}^M e^{i\alpha_{JM}}$ ,  $b_J^M e^{i\beta_{JM}}$ . (11)

Here,  $\alpha_{JM}$  is the relative phase between  $a_{1J}^M$  and  $a_{2J}^M$ , and  $\beta_{JM}$  is the relative phase between  $a_{1J}^M$  and  $b_J^M$ . It should be noted that when only one decay mode is contributed, the relative phase does not appear, and its own phase disappears in the form of modulus in the branching ratio calculations, so there is no need for special definition. The numerical results concerning the branching ratio were obtained from Monte Carlo simulations, and all experimental inputs were extracted from PDG [29]. Each process inputs a large number of random samples to ensure that the distribution of numerical results comprises at least 10000 sets of valid results. A more detailed discussion is provided below. The branching ratio is calculated using the fundamental two-body decay formula, which can be expressed as

$$\mathcal{B}(\chi_{cJ} \to M_1 M_2) = \frac{|\vec{p}|}{8\pi M_{\chi_{cJ}}^2 \Gamma_{\chi_{cJ}}} \left| \mathcal{A}(\chi_{cJ} \to M_1 M_2) \right|^2, \quad (12)$$

where  $\Gamma_{\chi_{cJ}}$  is the decay width of the  $\chi_{cJ}$  meson, and the center-of-mass momentum is expressed as  $|\vec{p}| \equiv \frac{\sqrt{[M_{\chi_{cJ}}^2 - (m_{M_1} + m_{M_2})^2][M_{\chi_{cJ}}^2 - (m_{M_1} - m_{M_2})^2]}}{2M_{\chi_{cJ}}}$ .

## B. Numerical results for $\chi_{cJ} \rightarrow PP$ decays

Numerical results for  $\chi_{cJ} \rightarrow PP$  decays are reported in this section. The experimental branching ratios are provided in the second column of Table 2 for  $\chi_{c0}$  decays and Table 3 for  $\chi_{c2}$  decays from PDG [29]. Based on SU(3) symmetry and breaking amplitudes, we obtained and analyzed two sets of branching ratio results for  $\chi_{cJ} \rightarrow PP$  decays. The results considering SU(3) symmetry are shown in the third columns of Table 2 and Table 3, while those incorporating breaking effects are listed in the fourth columns. Furthermore, the decays of  $\chi_{c1}$  ( $J^{PC} = 1^{++}$ ) into two pseudoscalar mesons are forbidden by spin-parity conservation and helicity selection rule; therefore, they were not considered in this analysis.

First, let us analyze the results within the SU(3) flavor symmetry framework. The experimental data related to the  $\chi_{c0} \to K^+K^-$ ,  $\eta\eta, \eta\eta', \eta'\eta'$  and  $\chi_{c2} \to K^+K^-, \eta\eta, \eta\eta'$ ,  $\eta'\eta'$  decays can be explained within  $1\sigma$  error. After using the constrained non-perturbative parameters from the data related to  $\chi_{c0} \to K^+K^-, \eta\eta, \eta\eta', \eta'\eta'$  or  $\chi_{c2} \to K^+K^-, \eta\eta$ ,  $\eta\eta',\eta'\eta'$  decays, the predicted branching ratios of the  $\chi_{c0} \rightarrow \pi\pi$  and  $\chi_{c2} \rightarrow \pi\pi$  decays slightly deviate from their experimental data within  $1\sigma$  error. Nevertheless, they could be consistent within approximately  $2\sigma$  or  $3\sigma$  error bars. All predicted branching ratios also exhibit a relatively accurate range. This suggests that the SU(3) flavor symmetry achieves good conformity with the overall decay modes. In particular, the  $a_{1J}^P$  term exhibits dominance across most decay channels. The maximum value of the ratio  $\frac{a_{2J}^P}{a_{1J}^P}$  reaches 37% for the  $\chi_{c0}$  decays and 45% for the  $\chi_{c2}$  decays, and they are supported by supression from

doubly OZI [35, 36]. Within the SU(3) flavor symmetry framework, the amplitude form of  $\eta\eta'$  has only the  $a_{2J}^P$  component, which also conforms to the result of suppression.

After considering the SU(3) flavor breaking effects, as listed in the fourth columns of Tables 2 and 3, all experimental data related to both  $\chi_{c0}$  and  $\chi_{c2}$  decays, including the  $\pi\pi$  modes, can be explained within  $1\sigma$  error bar. In terms of  $\frac{b_J^M}{a_{1J}^M}$  as the breaking ratio, the maximum value is 14% in the  $\chi_{c0}$  decays and 22% in the  $\chi_{c2}$  decays. Although the contributions from the  $b_J^M$  term are small compared to those of  $a_{2J}^P$ , they provide better fits for the relative experimental data within  $1\sigma$  error. As a result, there is an increased error range for certain channels, such as  $\chi_{c2} \to K^+K^-$  and  $\chi_{c2} \to K^0\bar{K}^0$ . It implies that while the breaking contributions are small, they should not be ig-

The allowed ranges of the non-perturbative parameters  $a_{1J}^P$ ,  $a_{2J}^P$ ,  $b_J^P$ ,  $|\alpha_{JP}|$ , and  $|\beta_{JP}|$  are listed in the last five lines of Tables 2 and 3. Please note that their allowed values are interrelated. These interrelations are shown in Fig. 2.

Recent measurements of BESIII [37] reported the following precision branching ratios:

$$\mathcal{B}(\chi_{c0} \to K^+ K^-) = (6.36 \pm 0.15) \times 10^{-3},$$

$$\mathcal{B}(\chi_{c0} \to \pi^+ \pi^-) = (6.06 \pm 0.15) \times 10^{-3},$$

$$\mathcal{B}(\chi_{c2} \to K^+ K^-) = (1.22 \pm 0.03) \times 10^{-3},$$

$$\mathcal{B}(\chi_{c2} \to \pi^+ \pi^-) = (1.61 \pm 0.04) \times 10^{-3},$$

**Table 2.** Branching ratios for  $\chi_{c0} \rightarrow PP$  decays within  $1\sigma$  error (in units of  $10^{-3}$ ).

|                                          | Exp. data [29]  | Symmetry                    | Including breaking           |
|------------------------------------------|-----------------|-----------------------------|------------------------------|
| $\mathcal{B}(\chi_{c0}\to\pi^+\pi^-)$    | •••             | $6.33 \pm 0.33$             | $5.67 \pm 0.27$              |
| $\mathcal{B}(\chi_{c0}\to\pi^0\pi^0)$    | •••             | $3.17 \pm 0.16$             | $2.83 \pm 0.13$              |
| $\mathcal{B}(\chi_{c0} \to \pi\pi)$      | $8.50 \pm 0.40$ | $9.50 \pm 0.49^{\sharp}$    | $8.50 \pm 0.40$              |
| $\mathcal{B}(\chi_{c0} \to K^+ K^-)$     | $6.07 \pm 0.33$ | $6.08 \pm 0.32$             | $6.07 \pm 0.33$              |
| $\mathcal{B}(\chi_{c0}\to K^0\bar{K}^0)$ | •••             | $6.08 \pm 0.32$             | $6.07 \pm 0.33$              |
| $\mathcal{B}(\chi_{c0}\to K\bar{K})$     | •••             | $12.16 \pm 0.63$            | $12.14 \pm 0.66$             |
| $\mathcal{B}(\chi_{c0} \to \eta \eta)$   | $3.01 \pm 0.25$ | $2.91 \pm 0.15$             | $2.92 \pm 0.16$              |
| $\mathcal{B}(\chi_{c0} \to \eta \eta')$  | $0.09 \pm 0.01$ | $0.09 \pm 0.01$             | $0.09 \pm 0.01$              |
| $\mathcal{B}(\chi_{c0} \to \eta' \eta')$ | $2.17 \pm 0.12$ | $2.17 \pm 0.12$             | $2.17 \pm 0.12$              |
| $a_{10}^{P} (10^{-2})$                   | •••             | $5.41 \pm 0.28$             | $5.30 \pm 0.27$              |
| $a_{20}^P (10^{-2})$                     |                 | $1.48 \pm 0.56$             | $1.12 \pm 1.04$              |
| $b_0^P (10^{-2})$                        | •••             | •••                         | $0.40 \pm 0.35$              |
| $ \alpha_{0P} $                          | •••             | $(119.75 \pm 9.74)^{\circ}$ | $(142.09 \pm 37.82)^{\circ}$ |
| $ eta_{0P} $                             |                 |                             | $(136.36 \pm 43.54)^{\circ}$ |

<sup>#</sup>indicates that experimental data were not used to derive the numerical results.

**Table 3.** Branching ratios for  $\chi_{c2} \rightarrow PP$  decays within  $1\sigma$  error (in units of  $10^{-4}$ ).

|                                          | Exp. data [29]   | Symmetry                    | Including breaking           |
|------------------------------------------|------------------|-----------------------------|------------------------------|
| $\mathcal{B}(\chi_{c2} \to \pi^+\pi^-)$  | •••              | 11.67 ± 0.47                | 15.13 ± 0.67                 |
| $\mathcal{B}(\chi_{c2}\to\pi^0\pi^0)$    | •••              | $5.83 \pm 0.24$             | $7.57 \pm 0.33$              |
| $\mathcal{B}(\chi_{c2} \to \pi\pi)$      | $22.70 \pm 1.00$ | $17.50 \pm 0.71^{\sharp}$   | $22.70 \pm 1.00$             |
| $\mathcal{B}(\chi_{c2} \to K^+K^-)$      | $10.20 \pm 1.50$ | $11.24 \pm 0.46$            | $10.20 \pm 1.50$             |
| $\mathcal{B}(\chi_{c2}\to K^0\bar{K}^0)$ | •••              | $11.24 \pm 0.46$            | $10.20 \pm 1.50$             |
| $\mathcal{B}(\chi_{c2} \to K\bar{K})$    | •••              | $22.48 \pm 0.91$            | $20.39 \pm 3.00$             |
| $\mathcal{B}(\chi_{c2} \to \eta \eta)$   | $5.50 \pm 0.50$  | $5.22 \pm 0.22$             | $5.42 \pm 0.42$              |
| $\mathcal{B}(\chi_{c2} \to \eta \eta')$  | $0.22 \pm 0.05$  | $0.22 \pm 0.05$             | $0.22 \pm 0.05$              |
| $\mathcal{B}(\chi_{c2} \to \eta' \eta')$ | $0.46 \pm 0.06$  | $0.46 \pm 0.06$             | $0.46 \pm 0.06$              |
| $a_{12}^P (10^{-2})$                     | •••              | $1.02 \pm 0.04$             | $1.03 \pm 0.08$              |
| $a_{22}^P (10^{-2})$                     | •••              | $0.35 \pm 0.11$             | $0.32 \pm 0.16$              |
| $b_2^P (10^{-2})$                        | •••              | •••                         | $0.14 \pm 0.08$              |
| $ \alpha_{2P} $                          | •••              | $(170.17 \pm 9.74)^{\circ}$ | $(165.58 \pm 14.32)^{\circ}$ |
| $ oldsymbol{eta}_{2P} $                  | •••              | •••                         | $(31.51 \pm 30.94)^{\circ}$  |

<sup>#</sup> indicates that experimental data were not used to derive the numerical results.

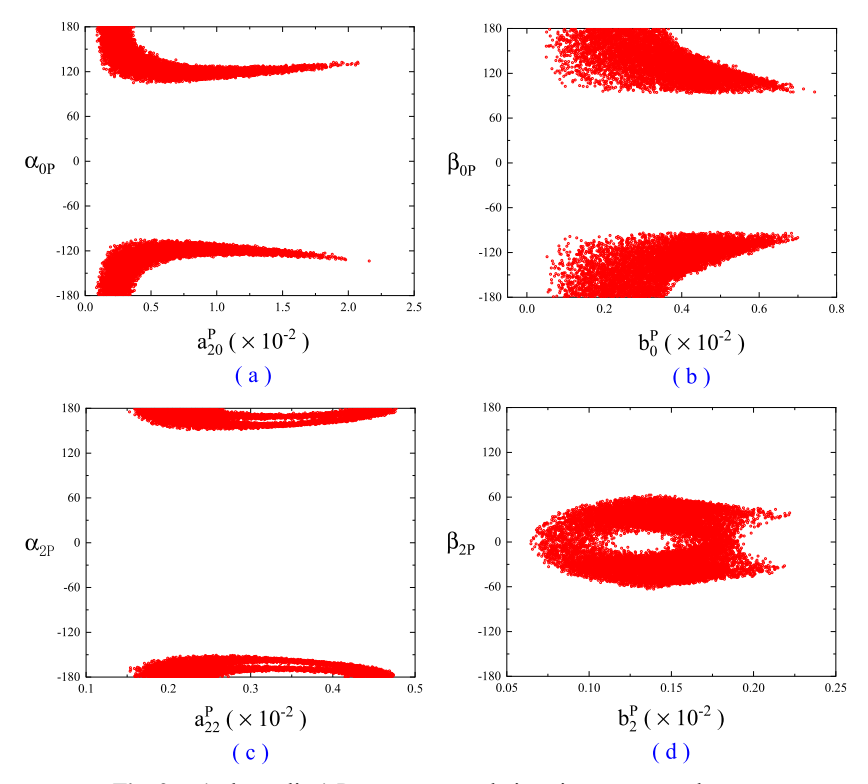


**Fig. 2.** (color online) Parameter correlations in  $\chi_{c0,2} \rightarrow PP$  decays.

which were used neither to constrain the non-perturbative coefficients nor to predict the not-yet-measured branching ratios in this study. Our predictions on  $\mathcal{B}(\chi_{c0,2} \to \pi^+\pi^-)$  are consistent with the above data within  $1\sigma$  error bar. The aforementioned experimental data related to  $\mathcal{B}(\chi_{c0} \to K^+K^-)$  or  $\mathcal{B}(\chi_{c2} \to K^+K^-)$  are consistent with those from PDG [29] within  $1\sigma$  or  $1.2\sigma$  error bars.

Several results from previous studies provide useful reference points. For instance, Ref. [16] proposed parametrization schemes to further understand the mechanisms that violate the OZI rule. These authors deepened the understanding of charmonium decay mechanisms by defining the relative strength r and some other physical quantities based on the SU(3) flavor approach. They

provided good fit results based on experimental data at the time as well as useful insights into the channels of isospin-0 light meson pairs. With the update of experimental measurements, we provide more theoretical predictions following the SU(3) flavor approach and using the latest experimental data. Our predicted results are expected to contribute to future research on  $\chi_{cJ} \rightarrow PP$  decays.

## C. Numerical results for $\chi_{cJ} \rightarrow VV$

 $\chi_{cJ} \rightarrow VV$  decays are similar to PP channels, although they present some key differences.  $\chi_{c1} \rightarrow VV$  decays are suppressed compared to  $\chi_{c0,2} \rightarrow VV$  decays because they violate the helicity selection rule [22], similar to their *PP* channels. However, interestingly,  $\chi_{c1} \rightarrow VV$ decays are not forbidden as initially expected. As experimental data have accumulated, further observations have revealed significant discrepancies among the data and the predictions based on the selection rule. One possible reason for the failure of the perturbative approach here could be that, although the charm quark is relatively heavy, it does not meet the mass threshold required by pQCD [26]. This suggests that there might be other mechanisms at play, such as higher-order contributions, final-state interactions, or long-distance effects, which could contribute to processes typically forbidden by the helicity selection rule. In any case, in this section we present the branching ratio results for  $\chi_{c0,1,2} \rightarrow VV$  based on the SU(3) flavor symmetry/breaking.

The experimental data are listed in the second columns of Tables 4, 5, and 6 for the  $\chi_{c0} \rightarrow VV$ ,  $\chi_{c1} \rightarrow VV$ , and  $\chi_{c2} \rightarrow VV$  decays, respectively. Our branching ratio predictions based on the SU(3) flavor symmetry are listed in the third columns of these tables, while predic-

tions including breaking effects are displayed in the fourth columns.

The results for  $\chi_{c0} \rightarrow VV$  with the SU(3) flavor symmetry show good agreement with present experimental data within  $1\sigma$  error, and their error ranges are small. However, for  $\chi_{c1} \rightarrow VV$  decays, the constrained  $a_{11}^V$  from  $\chi_{c1} \rightarrow K^{*0}\bar{K}^{*0}, \phi\omega, \omega\omega$  cannot explain the data of  $\chi_{c1} \rightarrow \phi\phi$  within  $1\sigma$  error. Nevertheless, one parameter,  $a_{11}^V$ , could explain all data if the error expands from  $1\sigma$  to  $1.1\sigma$ . Regarding  $\chi_{c2} \rightarrow VV$  decays, the four experimental data can be explained by one parameter,  $a_{22}^V$ , within  $1.5\sigma$  errors.

be explained by one parameter,  $a_{22}^V$ , within  $1.5\sigma$  errors. The maximum values of  $\frac{a_{2J}^V}{a_{1J}^V}$  across all datasets reach 30% for  $\chi_{c0}$  decays, 17% for  $\chi_{c1}$  decays, and 8% for  $\chi_{c2}$  decays. They indicate the dominant role of the  $a_{1J}^V$  amplitudes in  $\chi_{cJ} \rightarrow VV$  decays. Despite some theoretical shortcomings, the SU(3) flavor symmetry captures the essential correlations and still offers reasonable predictions. Thus, the results based on this symmetry reflect universal trends, with a small uncertainty in the data distribution, offering useful reference values.

Let us turn to the results including the SU(3) flavor breaking terms. All present experimental data for  $\chi_{c0,1,2} \rightarrow VV$  decays can be explained within  $1\sigma$  error bar if the SU(3) flavor breaking terms are included. The maximum ratio of breaking contributions, *i.e.*,  $\frac{b_J^V}{a_{IJ}^V}$ , is 55% for  $\chi_{c0}$  decays, 33% for  $\chi_{c1}$  decays, and 48% for  $\chi_{c2}$  decays. Compared to  $\chi_{cJ} \rightarrow PP$  decays, the allowed breaking contributions for  $\chi_{c0}$  and  $\chi_{c2}$  are more significant in VV decays at present, and they notably alter the distribution of branching ratios. The fundamental reason is that there are five relevant non-perturbative parameters and only four experimental data in  $\chi_{c0/c1/c2} \rightarrow VV$  decays, and the four

**Table 4.** Branching ratios for  $\chi_{c0} \to VV$  decays within  $1\sigma$  error (in units of  $10^{-3}$ ).

|                                                  | Exp. data [29]    | Symmetry                     | Including breaking           |
|--------------------------------------------------|-------------------|------------------------------|------------------------------|
| $\mathcal{B}(\chi_{c0} \to \rho^+ \rho^-)$       | •••               | $2.04 \pm 0.37$              | $2.28 \pm 1.56$              |
| $\mathcal{B}(\chi_{c0} \to \rho^0 \rho^0)$       | •••               | $1.02 \pm 0.18$              | $1.14 \pm 0.78$              |
| $\mathcal{B}(\chi_{c0} \to \rho \rho)$           | •••               | $3.06 \pm 0.55$              | $3.42 \pm 2.33$              |
| $\mathcal{B}(\chi_{c0} \to K^{*+}K^{*-})$        | •••               | $1.95 \pm 0.35$              | $1.70 \pm 0.60$              |
| $\mathcal{B}(\chi_{c0} \to K^{*0} \bar{K}^{*0})$ | $1.70\pm0.60$     | $1.95 \pm 0.35$              | $1.70 \pm 0.60$              |
| $\mathcal{B}(\chi_{c0} \to K^* \bar{K}^*)$       | •••               | $3.90 \pm 0.70$              | $3.40 \pm 1.20$              |
| $\mathcal{B}(\chi_{c0} 	o \phi\phi)$             | $0.848 \pm 0.031$ | $0.85 \pm 0.03$              | $0.85 \pm 0.03$              |
| $\mathcal{B}(\chi_{c0} 	o \phi\omega)$           | $0.142 \pm 0.013$ | $0.142 \pm 0.013$            | $0.142 \pm 0.013$            |
| $\mathcal{B}(\chi_{c0} \to \omega\omega)$        | $0.97 \pm 0.11$   | $0.97 \pm 0.11$              | $0.97 \pm 0.11$              |
| $a_{10}^{V} (10^{-2})$                           | •••               | $3.24 \pm 0.37$              | $2.98 \pm 0.85$              |
| $a_{20}^V (10^{-2})$                             | •••               | $0.86 \pm 0.06$              | $0.85 \pm 0.14$              |
| $b_0^V (10^{-2})$                                | •••               |                              | $0.78 \pm 0.78$              |
| $ lpha_{0V} $                                    | •••               | $(106.57 \pm 16.04)^{\circ}$ | $(120.89 \pm 59.01)^{\circ}$ |
| $ oldsymbol{eta}_{0V} $                          |                   |                              | $(90.00 \pm 90.00)^{\circ}$  |

**Table 5.** Branching ratios for  $\chi_{c1} \rightarrow VV$  decays within  $1\sigma$  error (in units of  $10^{-4}$ ).

|                                                | Exp. data [29]   | Symmetry                     | Including breaking           |
|------------------------------------------------|------------------|------------------------------|------------------------------|
| $\mathcal{B}(\chi_{c1} \to \rho^+ \rho^-)$     |                  | $12.35 \pm 1.92$             | $15.18 \pm 4.96$             |
| $\mathcal{B}(\chi_{c1}\to\rho^0\rho^0)$        |                  | $6.17 \pm 0.96$              | $7.59 \pm 2.48$              |
| $\mathcal{B}(\chi_{c1} \to \rho \rho)$         |                  | $18.52 \pm 2.87$             | $22.77 \pm 7.43$             |
| $\mathcal{B}(\chi_{c1} \to K^{*+}K^{*-})$      |                  | $11.85 \pm 1.84$             | $13.22 \pm 3.21$             |
| $\mathcal{B}(\chi_{c1}\to K^{*0}\bar{K}^{*0})$ | $14.00 \pm 4.00$ | $11.84 \pm 1.84$             | $13.20 \pm 3.20$             |
| $\mathcal{B}(\chi_{c1} \to K^* \bar{K}^*)$     |                  | $23.69 \pm 3.68$             | $26.42 \pm 6.41$             |
| $\mathcal{B}(\chi_{c1} \to \phi \phi)$         | $4.26 \pm 0.21$  | $5.24 \pm 0.73^{\sharp}$     | $4.26 \pm 0.21$              |
| $\mathcal{B}(\chi_{c1} \to \phi\omega)$        | $0.27 \pm 0.04$  | $0.27 \pm 0.04$              | $0.27 \pm 0.04$              |
| $\mathcal{B}(\chi_{c1} \to \omega \omega)$     | $5.70 \pm 0.70$  | $5.70 \pm 0.70$              | $5.70 \pm 0.70$              |
| $a_{11}^{V} (10^{-3})$                         |                  | $6.96 \pm 0.54$              | $7.59 \pm 1.17$              |
| $a_{21}^V (10^{-3})$                           | •••              | $1.06 \pm 0.10$              | $1.05 \pm 0.19$              |
| $b_1^V (10^{-3})$                              |                  | •••                          | $1.17\pm1.14$                |
| $ lpha_{1V} $                                  |                  | $(105.42 \pm 28.65)^{\circ}$ | $(134.65 \pm 45.26)^{\circ}$ |
| $ oldsymbol{eta}_{1V} $                        | •••              |                              | $(47.56 \pm 47.56)^{\circ}$  |

<sup>#</sup> indicates that experimental data were not used to derive the numerical results.

**Table 6.** Branching ratios for  $\chi_{c2} \to VV$  decays within  $1\sigma$  error (in units of  $10^{-4}$ ).

|                                               | Exp. data [29]    | Symmetry                    | Including breaking           |
|-----------------------------------------------|-------------------|-----------------------------|------------------------------|
| $\mathcal{B}(\chi_{c2} \to \rho^+ \rho^-)$    | •••               | $27.08 \pm 5.20$            | $18.38 \pm 8.04$             |
| $\mathcal{B}(\chi_{c2} \to \rho^0 \rho^0)$    | •••               | $13.54 \pm 2.60$            | $9.19 \pm 4.02$              |
| $\mathcal{B}(\chi_{c2} \to \rho \rho)$        | •••               | $40.62 \pm 7.80$            | $27.57 \pm 12.06$            |
| $\mathcal{B}(\chi_{c2} \to K^{*+}K^{*-})$     | •••               | $26.04 \pm 5.00$            | $20.39 \pm 7.37$             |
| $\mathcal{B}(\chi_{c2} 	o K^{*0} ar{K}^{*0})$ | $22.00 \pm 9.00$  | $26.00 \pm 4.99$            | $20.36 \pm 7.36$             |
| $\mathcal{B}(\chi_{c2} \to K^* \bar{K}^*)$    | •••               | $52.03 \pm 9.99$            | $40.76 \pm 14.74$            |
| $\mathcal{B}(\chi_{c2} 	o \phi\phi)$          | $12.30 \pm 0.70$  | $12.30 \pm 0.70$            | $12.30 \pm 0.70$             |
| $\mathcal{B}(\chi_{c2} 	o \phi\omega)$        | $0.097 \pm 0.028$ | $0.097 \pm 0.028$           | $0.097 \pm 0.028$            |
| $\mathcal{B}(\chi_{c2} \to \omega\omega)$     | $8.60 \pm 1.00$   | $13.57 \pm 2.36^{\sharp}$   | $8.60 \pm 1.00$              |
| $a_{12}^V (10^{-3})$                          | •••               | $16.31 \pm 1.87$            | $13.73 \pm 3.09$             |
| $a_{22}^V (10^{-3})$                          | •••               | $0.98 \pm 0.17$             | $0.98 \pm 0.48$              |
| $b_2^V (10^{-3})$                             | •••               | •••                         | $2.92 \pm 2.59$              |
| $ lpha_{2V} $                                 | •••               | $(90.00 \pm 90.00)^{\circ}$ | $(90.00 \pm 90.00)^{\circ}$  |
| $ oldsymbol{eta}_{2V} $                       | •••               | •••                         | $(131.21 \pm 48.70)^{\circ}$ |

<sup>#</sup>indicates that experimental data were not used to derive the numerical results.

experimental data are not enough to set constraints on the five parameters. Therefore,  $b_J^V$  and  $\beta_{JV}$  are not well determined owing to the lack of experimental values for the  $\rho\rho$  channels, making it difficult to accurately predict the contribution of the breaking. For decays of  $\chi_{c2} \to VV$ , the constraints on parameters are further weakened owing to the large error of the  $K^{*0}\bar{K}^{*0}$  channel, for example in terms of  $a_{22}^V$  and  $\alpha_{2V}$ . Therefore, as the breaking contributions are included, the uncertainty in the predicted results becomes larger, especially for some decay channels such as  $\chi_{c0,1,2} \to \rho\rho$  and  $\chi_{c1,2} \to K^*\bar{K}^*$ . However, the  $\phi\phi$ ,  $\phi\omega$ ,

and  $\omega\omega$  channels exhibit good agreement and still offer valuable insights. The predicted results reflect the basic distribution range and provide useful early reference points. Following the same approach, the error ranges will decrease in the future with more experimental inputs.

Figure 3 shows the relationship between the constrained symmetry/breaking parameters  $(a_{2J}^V, b_J^V)$  and their associated phases  $(\alpha_{JV}, \beta_{JV})$ . Note that, after satisfying all relevant experimental data, the allowed spaces are still large. This may indicate that the non-perturbative coefficients have not been properly limited by present experi-

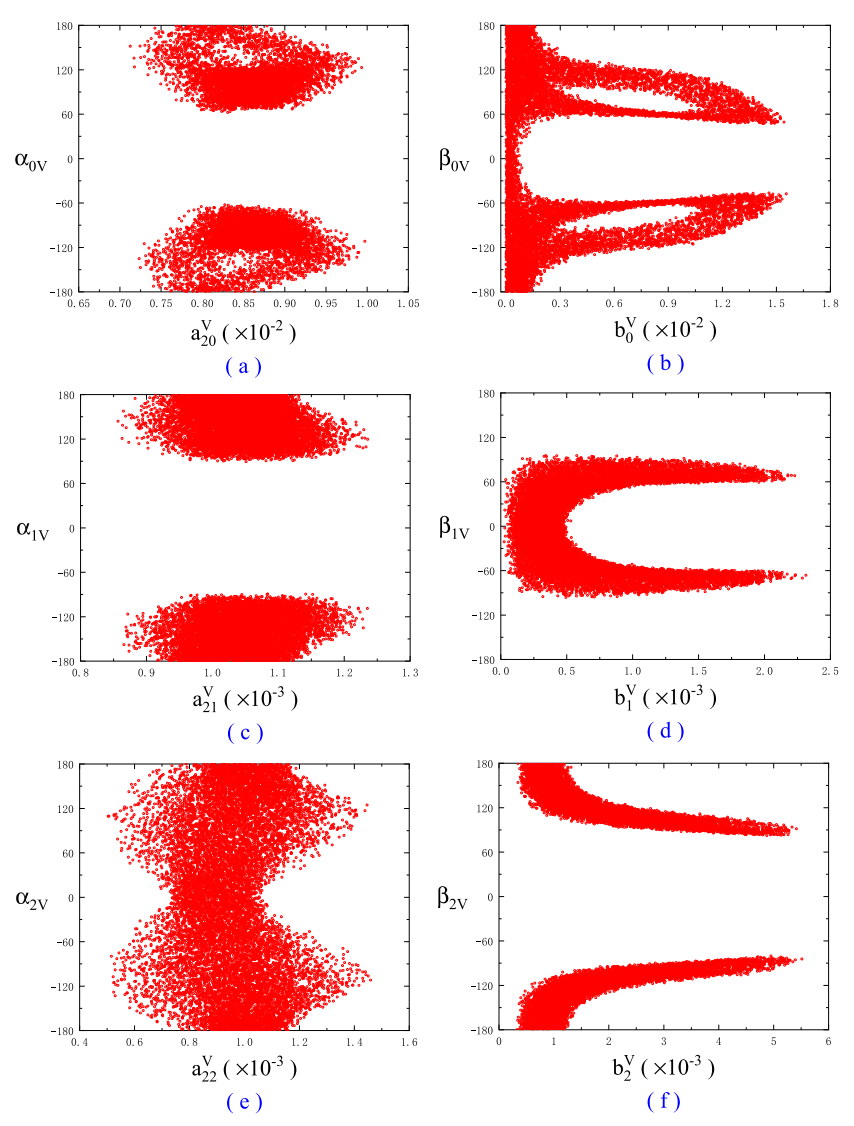


**Fig. 3.** (color online) Parameter correlations in  $\chi_{c0,1,2} \rightarrow VV$  decays.

mental data within  $1\sigma$  error, further leading to an increase in the uncertainty range of some predicted branching ratio results.

Next, we discuss the non-yet-measured  $\chi_{cJ} \to \rho \rho$  decays. Previous studies reported that  $\mathcal{B}(\chi_{c0} \to \rho \rho) = (1.88 \pm 1.80) \times 10^{-3}$  and  $\mathcal{B}(\chi_{c2} \to \rho \rho) = (2.41 \pm 2.22) \times 10^{-3}$  in a general factorization scheme [25], and  $\mathcal{B}(\chi_{c1} \to \rho \rho)$  lies in [26,54]×10<sup>-4</sup> according to the intermediate meson loop contributions [26]. Our predictions are consistent with these results, and the  $\chi_{c1,2} \to \rho \rho$  decays exhibit relatively more precise ranges.

## **III.** $\chi_{cJ} \rightarrow PV, PT$ **DECAYS**

## **A.** Amplitude relations of $\chi_{cJ} \to PV$ and PT decays The decays of $\chi_{c0,2} \to PV$ and PT are suppressed by

the helicity selection rule. Furthermore, the *G*-parity or isospin conservation exists in these decays. Rendering conventional theoretical approaches is significantly challenging when it comes to addressing these suppressed decay modes. Owing to the helicity selection rule, the number of  $\chi_{cJ} \rightarrow PV, PT$  decay channels measured is small. The decays of  $\chi_{c0} \rightarrow PV$  and PT vanish owing to charmed vector current conservation and parity conservation forbidden by spin-parity conservation [38]. Moreover, they lack robust phenomenological constraints in the absence of experimental observable values [38, 39]. Therefore, only  $\chi_{c1}$  and  $\chi_{c2}$  decays are discussed in this section.

The SU(3) flavor symmetry/breaking approach is still used to obtain the branching ratio results of  $\chi_{cJ} \rightarrow PV$  and PT. The tensor meson octet states can be expressed as

$$T = \begin{pmatrix} \frac{a_2^0}{\sqrt{2}} + \frac{f_2^8}{\sqrt{6}} + \frac{f_2^0}{\sqrt{3}} & a_2^+ & K_2^{*+} \\ a_2^- & -\frac{a_2^0}{\sqrt{2}} + \frac{f_2^8}{\sqrt{6}} + \frac{f_2^0}{\sqrt{3}} & K_2^{*0} \\ K_2^{*-} & \bar{K}_2^{*0} & -\frac{2f_2^8}{\sqrt{6}} + \frac{f_2^0}{\sqrt{3}} \end{pmatrix}.$$

$$(13)$$

The mixing of  $f_2$ - $f'_2$  is described as

$$f_2 = \left( f_2^8 \cos \theta_T - f_2^0 \sin \theta_T \right), \tag{14}$$

$$f_2' = (f_2^8 \sin \theta_T + f_2^0 \cos \theta_T),$$
 (15)

and the results for  $\theta_T = (27 \pm 1)^\circ$  were selected from PDG [29]. Following the same theory described in Sec. II.A, we derived the decay amplitudes for *PT* and *PV* channels; they are listed in Table 7.

#### **B.** Numerical results for $\chi_{cJ} \rightarrow PV$ decays

The neutral PV channels for  $\chi_{c1}$  and  $\chi_{c2}$  decays, such as  $\pi^0\rho^0$  and  $\eta\omega$ , are forbidden by C-parity conservation. Furthermore, the  $\chi_{c2} \to PV$  decays are not only suppressed by the helicity selection rule but also suffer from G-parity or isospin/U-spin conservation [26]. Although these processes lack experimental observations, we still provide phenomenological predictions under existing models. It is worth mentioning that many PV and PT processes are difficult to effectively constrain theoretically, so we only provide numerical predictions based on relevant experimental data from PDG [29]. Moreover, the

experimental limits are significantly less than the theoretical non-perturbative parameters that need to be determined, and effective results cannot be obtained without additional constraints. Therefore, in the following, we refer to the parameter ratios of *PP* and *VV* processes to limit the upper bounds of parameters in order to obtain early prediction results.

For  $\chi_{c1} \rightarrow PV$  decays, only two modes of  $\chi_{c1} \rightarrow K\bar{K}^*$  have been measured [29]. Their experimental data are listed in the second column of Table 8. In these decays, relevant non-perturbative coefficients, namely  $a_{21}^{PV}$  and  $b_{1}^{PV}$ , lack effective experimental constraints. Concerning our results for  $\chi_{cJ} \rightarrow PP, VV$ , the constraints of  $\frac{a_{21}^{PV}}{a_{11}^{PV}} \le 45\%$  and  $\frac{b_{1}^{PV}}{a_{11}^{PV}} \le 55\%$  were imposed to obtain the predictions. The branching ratio prediction results for  $\chi_{c1} \rightarrow PV$  via SU(3) flavor symmetry are shown in the third column of Table 8, while those including the breaking results are presented in the last column of Table 8. From Table 8, it can be concluded that many errors of our predictions are notably large, given that there are no other experimental data to constrain  $a_{21}^{PV}$ ,  $b_{1}^{PV}$  and the corresponding two phases.

For  $\chi_{c2} \to PV$  decays, three decay modes, namely  $\chi_{c2} \to K^{\pm}K^{*\mp}, K^0\bar{K}^{*0} + c.c., \pi^{\pm}\rho^{\mp}$ , have been measured [29]. They are listed in the second column of Table 9. As shown in the third column of IX, within the SU(3) flavor symmetry framework, the constrained  $a_{12}^{PV}$  from  $\mathcal{B}(\chi_{c2} \to K^{\pm}K^{*\mp}, K^0\bar{K}^{*0} + c.c.)$  cannot explain the experimental data for  $\mathcal{B}(\chi_{c2} \to \pi^{\pm}\rho^{\mp})$ . Furthermore, according to the SU(3) flavor symmetry,  $\mathcal{B}(\chi_{c2} \to \pi^{\pm}\rho^{\mp})$  is on the order of

| <b>Table 7.</b> $SU(3)$ symmetry and breaking amplitudes of $\chi_{cJ} \rightarrow PV$ and $\chi_{cJ} \rightarrow PV$ | Table 7. | SU(3) symmetry and bre | aking amplitudes of $\chi_c$ | $J \to PV$ and $\chi_{cJ} \to PT$ . |
|-----------------------------------------------------------------------------------------------------------------------|----------|------------------------|------------------------------|-------------------------------------|
|-----------------------------------------------------------------------------------------------------------------------|----------|------------------------|------------------------------|-------------------------------------|

| Decay modes                                           | Symmetry amplitudes                                                                       | Breaking amplitudes                                                                |
|-------------------------------------------------------|-------------------------------------------------------------------------------------------|------------------------------------------------------------------------------------|
| $\chi_{cJ} \to \pi^+ \rho^- / \pi^+ a_2^-$            | $2a_{1J}^{MM}$                                                                            | $2b_J^{MM}$                                                                        |
| $\chi_{cJ} \rightarrow \pi^- \rho^+ / \pi^- a_2^+$    | $2a_{1J}^{MM}$                                                                            | $2b_J^{MM}$                                                                        |
| $\chi_{cJ} \to K^+ K^{*-} / K^- K_2^{*+}$             | $2a_{1J}^{MM}$                                                                            | $-b_J^{MM}$                                                                        |
| $\chi_{cJ} \to K^- K^{*+} / K^- K_2^{*+}$             | $2a_{1J}^{MM}$                                                                            | $-b_J^{MM}$                                                                        |
| $\chi_{cJ} \to K^0 \bar{K}^{*0} / K^0 \bar{K}_2^{*0}$ | $2a_{1J}^{MM}$                                                                            | $-b_J^{MM}$                                                                        |
| $\chi_{cJ} \to \bar{K}^0 K^{*0} / \bar{K}^0 K_2^{*0}$ | $2a_{1J}^{MM}$                                                                            | $-b_J^{MM}$                                                                        |
| $\chi_{cJ} \rightarrow \pi^0 \rho^0 / \pi^0 a_2^0$    | $2a_{1J}^{MM}$                                                                            | $2b_J^{MM}$                                                                        |
| $\chi_{cJ} \to \eta_1 \omega_1/\eta_1 f_2^0$          | $2a_{1J}^{MM} + 6a_{2J}^{MM}$                                                             | 0                                                                                  |
| $\chi_{cJ} \to \eta_1 \omega_8/\eta_1 f_2^8$          | 0                                                                                         | $2\sqrt{2}b_J^{MM}$                                                                |
| $\chi_{cJ} \to \eta_8 \omega_1/\eta_8 f_2^0$          | 0                                                                                         | $2\sqrt{2}b_J^{MM}$                                                                |
| $\chi_{cJ}  ightarrow \eta_8 \omega_8/\eta_8 f_2^8$   | $2a_{1J}^{MM}$                                                                            | $-2b_J^{MM}$                                                                       |
| $\chi_{cJ} \to \eta \phi/\eta f_2'$                   | $2a_{1J}^{MM}(\cos(\theta_P - \theta_{V/T})) + 6a_{2J}^{MM}\sin\theta_P\sin\theta_{V/T}$  | $-2b_J^{MM}(\cos\theta_P\cos\theta_{V/T} + \sqrt{2}\sin(\theta_P + \theta_{V/T}))$ |
| $\chi_{cJ} \to \eta \omega / \eta f_2$                | $2a_{1J}^{MM}(-\sin(\theta_P - \theta_{V/T})) - 6a_{2J}^{MM}\sin\theta_P\cos\theta_{V/T}$ | $-2b_J^{MM}(\cos\theta_P\sin\theta_{V/T}-\sqrt{2}\cos(\theta_P+\theta_{V/T}))$     |
| $\chi_{cJ} \rightarrow \eta' \phi / \eta' f_2'$       | $2a_{1J}^{MM}(\sin(\theta_P - \theta_{V/T})) - 6a_{2J}^{MM}\cos\theta_P\sin\theta_{V/T}$  | $-2b_J^{MM}(\sin\theta_P\cos\theta_{V/T}-\sqrt{2}\cos(\theta_P+\theta_{V/T}))$     |
| $\chi_{cJ} \to \eta' \omega / \eta' f_2$              | $2a_{1J}^{MM}(\cos(\theta_P - \theta_{V/T})) + 6a_{2J}^{MM}\cos\theta_P\cos\theta_{V/T}$  | $-2b_J^{MM}(\sin\theta_P\sin\theta_{V/T}-\sqrt{2}\sin(\theta_P+\theta_{V/T}))$     |

| Table 8.  | Branching ratios for $\chi_{c1} \rightarrow PV$    | decays within $1\sigma$ error | (in units of $10^{-3}$ ) |
|-----------|----------------------------------------------------|-------------------------------|--------------------------|
| i abic o. | Dranching ratios for $\chi_{c1} \rightarrow i \nu$ | accays within 10 circl        | (III uiiits of 10        |

|                                                      | Exp. data [29]  | Symmetry                    | Including breaking          |
|------------------------------------------------------|-----------------|-----------------------------|-----------------------------|
| $\mathcal{B}(\chi_{c1} \to \pi^{\pm} \rho^{\mp})$    | •••             | 1.12±0.11                   | $2.78 \pm 2.65$             |
| $\mathcal{B}(\chi_{c1} \to \pi^0 \rho^0)$            | •••             | $0.56 \pm 0.05$             | $1.39 \pm 1.32$             |
| $\mathcal{B}(\chi_{c1} 	o K^{\pm}K^{*\mp})$          | $1.21 \pm 0.23$ | $1.08 \pm 0.10$             | $1.08 \pm 0.10$             |
| $\mathcal{B}(\chi_{c1} \to K^0 \bar{K}^{*0} + c.c.)$ | $1.03 \pm 0.15$ | $1.08 \pm 0.10$             | $1.08 \pm 0.10$             |
| $\mathcal{B}(\chi_{c1} 	o \eta \phi)$                | •••             | $0.21 \pm 0.17$             | $0.40 \pm 0.40$             |
| $\mathcal{B}(\chi_{c1} 	o \eta \omega)$              | •••             | $0.47 \pm 0.34$             | $1.16 \pm 1.15$             |
| $\mathcal{B}(\chi_{c1} \to \eta' \phi)$              | •••             | $0.64 \pm 0.64$             | $0.87 \pm 0.87$             |
| $\mathcal{B}(\chi_{c1} \to \eta'\omega)$             | •••             | $0.77 \pm 0.77$             | $1.93 \pm 1.93$             |
| $a_{11}^{PV} (10^{-3})$                              | •••             | $4.68 \pm 0.32$             | $5.12 \pm 1.65$             |
| $a_{21}^{PV} (10^{-3})$                              | •••             | $1.11 \pm 1.11$             | $1.46 \pm 1.46$             |
| $b_1^{PV} (10^{-3})$                                 | •••             |                             | $1.85 \pm 1.85$             |
| $ lpha_{1PV} $                                       | •••             | $(90.00 \pm 90.00)^{\circ}$ | $(90.00 \pm 90.00)^{\circ}$ |
| $ oldsymbol{eta}_{1PV} $                             | •••             | ***                         | $(90.00 \pm 90.00)^{\circ}$ |

**Table 9.** Branching ratios for  $\chi_{c2} \rightarrow PV$  decays within  $1\sigma$  error (in units of  $10^{-4}$ ).

|                                                      | Exp. data [29]  | Symmetry                    | Including breaking           |
|------------------------------------------------------|-----------------|-----------------------------|------------------------------|
| $\mathcal{B}(\chi_{c2} \to \pi^{\pm} \rho^{\mp})$    | $0.06 \pm 0.04$ | $1.45 \pm 0.15^{\sharp}$    | $0.06 \pm 0.04$              |
| $\mathcal{B}(\chi_{c2}\to\pi^0\rho^0)$               | •••             | $0.73 \pm 0.08$             | $0.03 \pm 0.02$              |
| $\mathcal{B}(\chi_{c2} \to K^{\pm}K^{*\mp})$         | $1.46 \pm 0.21$ | $1.40 \pm 0.15$             | $1.40\pm0.15$                |
| $\mathcal{B}(\chi_{c2} \to K^0 \bar{K}^{*0} + c.c.)$ | $1.27\pm0.27$   | $1.40 \pm 0.15$             | $1.40\pm0.15$                |
| $\mathcal{B}(\chi_{c2} 	o \eta \phi)$                | •••             | $0.28 \pm 0.23$             | $0.91 \pm 0.48$              |
| $\mathcal{B}(\chi_{c2} 	o \eta \omega)$              | •••             | $0.59 \pm 0.43$             | $0.09 \pm 0.09$              |
| $\mathcal{B}(\chi_{c2} \to \eta' \phi)$              |                 | $0.81 \pm 0.81$             | $1.55 \pm 1.25$              |
| $\mathcal{B}(\chi_{c2} \to \eta'\omega)$             |                 | $1.01 \pm 1.01$             | $0.31 \pm 0.31$              |
| $a_{12}^{PV} (10^{-3})$                              | •••             | $2.60 \pm 0.19$             | $1.91 \pm 0.18$              |
| $a_{22}^{PV}$ (10 <sup>-3</sup> )                    | •••             | $0.61 \pm 0.61$             | $0.46 \pm 0.46$              |
| $b_2^{PV} (10^{-3})$                                 | •••             | •••                         | $1.38 \pm 0.21$              |
| $ lpha_{2PV} $                                       |                 | $(90.00 \pm 90.00)^{\circ}$ | $(90.00 \pm 90.00)^{\circ}$  |
| $ eta_{2PV} $                                        | ***             | •••                         | $(169.60 \pm 10.31)^{\circ}$ |

<sup>#</sup>indicates that experimental data were not used to derive the numerical results.

 $O(10^{-4})$  and  $\mathcal{B}(\chi_{c2} \to \pi^0 \rho^0)$  is on the order of  $O(10^{-5})$ . If SU(3) flavor breaking is considered, their minimum allowed values are reduced by one order of magnitude. This means that a large breaking effect is needed to explain the experimental data for  $\mathcal{B}(\chi_{c2} \to \pi^{\pm} \rho^{\mp})$ .

plain the experimental data for  $\mathcal{B}(\chi_{c2} \to \pi^{\pm} \rho^{\mp})$ .

By considering the SU(3) flavor breaking and setting  $\frac{a_{22}^{PV}}{a_{12}^{PV}} \le 45\%$  as well as  $\frac{b_{2}^{PV}}{a_{12}^{PV}} \le 80\%$ , all three experimental data become simultaneously explained. Note that the three experimental data cannot be jointly explained when  $\frac{b_{2}^{PV}}{a_{12}^{PV}} \le 63\%$ . The predictions including the breaking contributions are presented in the last column of Table 9. Note that  $a_{12}^{PV}$ ,  $b_{2}^{PV}$ , and  $\beta_{2PV}$  are well constrained by three

experimental data within  $1\sigma$  error. Nevertheless, there is no constraint on  $a_{22}^{PV}$  and  $\alpha_{2PV}$  owing to the large error in some  $\chi_{c2} \to PV$  decays. Some predicted results fail to exhibit the anticipated theoretical suppression, given that this effect is obscured by substantial theoretically uncertainties. The branching ratios of  $\chi_{c2} \to \pi \rho$  and  $\chi_{c2} \to \eta \omega$  are significantly smaller compared to other decay channels when the flavor breaking effects are included. If we do not consider the theoretically forbidden scenario, this may be a signal that is suppressed by the helicity selection rule or other theories.

Moreover, note that the predicted branching ratios of  $K^{\pm}K^{*\mp}$  and  $K^{0}\bar{K}^{*0} + c.c.$  are completely consistent in the

symmetry and breaking cases. The main reason is that their shared amplitude structure  $2a_{1J}^{PV}-b_J^{PV}\mathrm{e}^{\mathrm{i}\beta_J^{PV}}$  and effective constraints on  $\left|2a_{1J}^{PV}-b_J^{PV}\mathrm{e}^{\mathrm{i}\beta_J^{PV}}\right|$  are obtained from the data of  $K^\pm K^{*\mp}$  and  $K^0 \bar{K}^{*0} + c.c.$  decays at present. A similar situation appears in the  $\chi_{c1,2} \to PT$  decays.

## C. Numerical results for $\chi_{cJ} \rightarrow PT$ decays

For PT decays, there is no C/G-parity conservation that imposes prohibitive constraints, and the helicity selection rule does not cause significant suppression. This theoretical landscape enables richer predictions for viable decay channels. Experimental measurements for  $\chi_{c1} \rightarrow PT$  and  $\chi_{c2} \rightarrow PT$  decays are compiled in the

second columns of Tables 10 and 11, respectively. SU(3) symmetry predictions are listed in the third columns, and the breaking cases are presented in the final columns.

The  $\eta f_2'$ ,  $\eta f_2$ ,  $\eta' f_2'$ , and  $\eta' f_2$  channels exhibit sensitivity to the  $a_{2J}^{PT}$  amplitude parameter. However, the absence of experimental constraints makes it difficult to determine the accuracy of  $a_{2J}^{PT}$  and  $b_J^{PT}$  in the simulations, especially because there are no experimental data in  $\chi_{c2} \to PT$  that can limit the range of  $a_{2J}^{PT}$ . To address this, we impose upper limits,  $\frac{a_{2J}^{PT}}{a_{1J}^{PT}} \le 45\%$  and  $\frac{b_J^{PT}}{a_{1J}^{PT}} \le 55\%$ , based on analysis of PP and VV channels.

Regarding  $\chi_{c1} \rightarrow PT$  decays, the  $\eta f_2$  channel provides

| Table 10. | Branching ratios for $\chi_{c1} \rightarrow PT$ | decays within $1\sigma$ error | (in units of $10^{-3}$ | ). |
|-----------|-------------------------------------------------|-------------------------------|------------------------|----|
|-----------|-------------------------------------------------|-------------------------------|------------------------|----|

|                                                        | Exp. data [29]  | Symmetry                    | Including breaking          |
|--------------------------------------------------------|-----------------|-----------------------------|-----------------------------|
| $\mathcal{B}(\chi_{c1} \to \pi^{\pm} a_2^{\mp})$       |                 | $1.42 \pm 0.04$             | $3.03 \pm 2.14$             |
| $\mathcal{B}(\chi_{c1}\to\pi^0a_2^0)$                  |                 | $0.71 \pm 0.02$             | $1.51 \pm 1.07$             |
| $\mathcal{B}(\chi_{c1} \to K^{\pm}K_2^{*\mp})$         | $1.61 \pm 0.31$ | $1.34 \pm 0.04$             | $1.34 \pm 0.04$             |
| $\mathcal{B}(\chi_{c1} \to K^0 \bar{K}_2^{*0} + c.c.)$ | $1.17 \pm 0.20$ | $1.33 \pm 0.04$             | $1.33 \pm 0.04$             |
| $\mathcal{B}(\chi_{c1} \to \eta f_2')$                 |                 | $0.23 \pm 0.03$             | $0.42 \pm 0.31$             |
| $\mathcal{B}(\chi_{c1} \to \eta f_2)$                  | $0.67 \pm 0.11$ | $0.61 \pm 0.05$             | $0.67 \pm 0.11$             |
| $\mathcal{B}(\chi_{c1} \to \eta' f_2')$                |                 | $0.60 \pm 0.07$             | $0.76 \pm 0.76$             |
| $\mathcal{B}(\chi_{c1} \to \eta' f_2)$                 |                 | $0.99 \pm 0.21$             | $1.49 \pm 1.49$             |
| $a_{11}^{PT} (10^{-3})$                                |                 | $5.54 \pm 0.20$             | $6.09 \pm 1.16$             |
| $a_{21}^{PT} \ (10^{-3})$                              | •••             | $1.18 \pm 0.25$             | $1.60 \pm 1.60$             |
| $b_1^{PT} (10^{-3})$                                   | •••             | •••                         | $1.92 \pm 1.92$             |
| $ lpha_{1PT} $                                         |                 | $(25.78 \pm 25.78)^{\circ}$ | $(90.00 \pm 90.00)^{\circ}$ |
| $ oldsymbol{eta}_{1PT} $                               |                 |                             | $(90.00 \pm 90.00)^{\circ}$ |

**Table 11.** Branching ratios for  $\chi_{c2} \to PT$  decays within  $1\sigma$  error (in units of  $10^{-3}$ ).

|                                                        | Exp. data [29]  | Symmetry                    | Including breaking          |
|--------------------------------------------------------|-----------------|-----------------------------|-----------------------------|
| $\mathcal{B}(\chi_{c2} \to \pi^{\pm} a_2^{\mp})$       | $1.80 \pm 0.60$ | $1.50 \pm 0.03$             | $2.16 \pm 0.24$             |
| $\mathcal{B}(\chi_{c2}\to\pi^0a_2^0)$                  | $1.31 \pm 0.35$ | $0.75 \pm 0.02^{\sharp}$    | $1.08 \pm 0.12$             |
| $\mathcal{B}(\chi_{c2} \to K^{\pm} K_2^{*\mp})$        | $1.51 \pm 0.13$ | $1.41 \pm 0.03$             | $1.41 \pm 0.03$             |
| $\mathcal{B}(\chi_{c2} \to K^0 \bar{K}_2^{*0} + c.c.)$ | $1.27 \pm 0.17$ | $1.41 \pm 0.03$             | $1.41 \pm 0.03$             |
| $\mathcal{B}(\chi_{c2} \to \eta f_2')$                 | •••             | $0.37 \pm 0.15$             | $0.45 \pm 0.36$             |
| $\mathcal{B}(\chi_{c2} \to \eta f_2)$                  | •••             | $0.41 \pm 0.25$             | $0.77 \pm 0.62$             |
| $\mathcal{B}(\chi_{c2} \to \eta' f_2')$                | •••             | $0.37 \pm 0.32$             | $0.81 \pm 0.81$             |
| $\mathcal{B}(\chi_{c2} \to \eta' f_2)$                 | •••             | $0.70 \pm 0.70$             | $1.59 \pm 1.59$             |
| $a_{12}^{PT} (10^{-3})$                                | •••             | $8.77 \pm 0.30$             | $9.10 \pm 0.70$             |
| $a_{22}^{PT} (10^{-3})$                                | •••             | $1.13 \pm 1.13$             | $2.19 \pm 2.19$             |
| $b_2^{PT}$ (10 <sup>-3</sup> )                         | •••             | •••                         | $2.86 \pm 2.14$             |
| $ lpha_{2PT} $                                         | •••             | $(90.00 \pm 90.00)^{\circ}$ | $(90.00 \pm 90.00)^{\circ}$ |
| $ eta_{2PT} $                                          | •••             | •••                         | $(43.54 \pm 43.54)^{\circ}$ |

<sup>#</sup>indicates that experimental data were not used to derive the numerical results

critical constraints on  $a_{21}^{PT}$  and  $\alpha_{1PT}$ , improving the accuracy of predicting  $\eta f_2'$ ,  $\eta' f_2'$ , and  $\eta' f_2$  channels in the SU(3) flavor symmetry case. After considering the SU(3) flavor breaking,  $a_{21}^{PT}$  and  $b_{1}^{PT}$  are not constrained well, and the corresponding phases  $\alpha_{1PT}$  and  $\beta_{1PT}$  are completely unrestricted. This causes large errors in  $\mathcal{B}(\chi_{c1} \to \pi^\pm a_2^\mp)$ ,  $\mathcal{B}(\chi_{c1} \to \pi^0 a_2^0)$ ,  $\mathcal{B}(\chi_{c1} \to \eta' f_2')$ , and  $\mathcal{B}(\chi_{c1} \to \eta' f_2)$ , and the measurements of these branching ratios could further constrain relevant non-perturbative coefficients.

Concerning  $\chi_{c2} \to PT$  decays, in the SU(3) flavor symmetry case, the experimental data related to  $\mathcal{B}(\chi_{c2} \to \pi^{\pm}a_2^{\mp})$ ,  $\mathcal{B}(\chi_{c2} \to K^{\pm}K_2^{*\mp})$ , and  $\mathcal{B}(\chi_{c2} \to K^0\bar{K}_2^{*0} + c.c.)$  establish a strong constraint on  $a_{12}^{PT}$ ; however, the data related to  $\mathcal{B}(\chi_{c2} \to \pi^0 a_2^0)$  cannot be jointly explained with the other three. Given that there is no experimental constraint on  $a_{22}^{PT}$  and  $\alpha_{2PT}$ , the sources of errors are increased and there are relatively large ranges of uncertainty in the  $\chi_{c2} \to \eta f_2'$ ,  $\eta f_2$ ,  $\eta' f_2'$ , and  $\eta' f_2$  channels.

After considering the SU(3) flavor breaking, all four experimental data related to the  $\chi_{c2} \rightarrow PT$  decays can be jointly explained within a  $1\sigma$  error bar. The current experimental data impose some restrictions on  $b_2^{PT}$  and  $\beta_{2PT}$ , but they are not strong. In fact, for all PV and PT processes, effective limitations have only been imposed on  $a_{1J}^{PV,PT}$  within the existing experimental constraints, which at least ensures that all predicted results reflect the basic characteristics of the decay channels.

#### IV. CONCLUSIONS

Previous measurements by BESIII were based on accumulated 448 million  $\psi(3686)$  decays [40], which allowed access to  $\chi_{cJ}$  decays through radiative decays  $\psi(3686) \rightarrow \gamma \chi_{cJ}$ . With a current data sample of 2.7 billion  $\psi(3686)$  events collected by the BESIII detector [5], a

more detailed analysis of two body  $\chi_{cJ}$  decays is now possible. This provides an opportunity to test the SU(3) symmetry and gain deeper insights into their decay mechanisms

In this study, we investigated the  $\chi_{c0,2} \rightarrow PP$ ,  $\chi_{c0,1,2} \rightarrow VV$ , and  $\chi_{c1,2} \rightarrow PV$ , PV, decays following the SU(3) flavor symmetry/breaking approach. We obtained the amplitude relations for the SU(3) flavor symmetry case and for the case including the SU(3) flavor breaking. Because of the advantages of the symmetry approach, inconclusive intermediate decay mechanisms can be avoided. All branching ratios, including the predicted results for not-yet-measured or not-well-measured channels, have been presented in this paper.

Our study shows that the SU(3) symmetry approach works well in the two body decays of charmonium states  $\chi_{cJ}$  at present. These states are typically difficult to compute using traditional QCD methods. Specifically,  $\chi_{cJ} \rightarrow \eta \eta'$  and  $\chi_{cJ} \rightarrow \omega \phi$  are doubly OZI-suppressed, resulting in branching ratios for these decays that are clearly smaller than those for the singly OZI-suppressed decays  $\chi_{cJ} \rightarrow \eta \eta$ ,  $\eta \eta'$ ,  $\omega \omega$ , and  $\phi \phi$  [20, 35, 36, 41]. Our results are consistent with the suppression of the  $\eta \eta'$  and  $\omega \phi$  channels in the contributions of  $a_{2J}^M$  and align well with experimental data for these channels.

Our predictions not only contribute to future experimental measurements but also offer valuable reference points for future theoretical studies that aim to refine these calculations. Furthermore, with the high luminosity of the current experiments [42–44], we can expect a continuous stream of interesting experimental results to emerge, including precise measurements of branching ratios and potentially new insights into the decay mechanisms of  $\chi_{cJ}$  decaying into meson pairs.

#### References

- [1] J. Z. Bai et al. (BES), Phys. Lett. B 550, 24 (2002)
- [2] M. Ablikim et al. (BESIII), Chin. Phys. C 37, 063001 (2013)
- [3] M. Ablikim *et al.* (BESIII), Chin. Phys. C **37**, 123001
- [4] M. Ablikim *et al.* (BESIII),, Chin. Phys. C **42**, 023001 (2018)
- [5] M. Ablikim et al. (BESIII), Chin. Phys. C 48, 093001 (2024)
- [6] M. Ablikim et al. (BES), Phys. Lett. B 630, 7 (2005)
- [7] A. V. Luchinsky, Phys. Atom. Nucl. **70**, 53 (2007)
- [8] G. S. Adams *et al.* (CLEO), Phys. Rev. D **75**, 071101 (2007)
- [9] D. M. Asner et al. (CLEO), Phys. Rev. D 79, 072007 (2009)
- [10] M. Ablikim *et al.* (BESIII), Phys. Rev. D **81**, 052005 (2010)
- [11] H. Chen and R. G. Ping, Phys. Rev. D 88, 034025 (2013)
- [12] F. Gross et al., Eur. Phys. J. C 83, 1125 (2023)
- [13] H. Y. Cheng and C. W. Chiang, Phys. Rev. D 81, 074021

- (2010)
- [14] H. Y. Cheng and C. W. Chiang, Phys. Rev. D 85, 034036(2012) [Erratum: Phys. Rev. D 85, 079903 (2012)]
- [15] J. Iizuka, Prog. Theor. Phys. Suppl. 37, 21 (1966)
- [16] Q. Zhao, Phys. Lett. B 659, 221 (2008)
- [17] C. E. Thomas, JHEP **10**, 026 (2007)
- [18] D. Y. Chen, J. He, X. Q. Li et al., Phys. Rev. D 81, 074006 (2010)
- [19] M. Ablikim et al. (BESIII), Phys. Rev. D 99, 012015 (2019)
- [20] M. Ablikim et al. (BESII), Phys. Rev. Lett. 107, 092001 (2011)
- [21] Q. Wang, G. Li, and Q. Zhao, Int. J. Mod. Phys. A 27, 1250135 (2012)
- [22] V. L. Chernyak and A. R. Zhitnitsky, Nucl. Phys. B 201, 492 (1982) [Erratum: Nucl. Phys. B 214, 547 (1983)]
- [23] W. E. Caswell and G. P. Lepage, Phys. Lett. B 167, 437 (1986)
- [24] N. Brambilla, A. Pineda, J. Soto et al., Nucl. Phys. B 566, 275 (2000)
- [25] Q. Zhao, Phys. Rev. D 72, 074001 (2005)

- [26] X. H. Liu and Q. Zhao, Phys. Rev. D 81, 014017 (2010)
- [27] H. Q. Zhou, R. G. Ping, and B. S. Zou, Phys. Lett. B **611**, 123 (2005)
- [28] N. Kivel, JHEP **07**, 065 (2024)
- [29] S. Navas et al. (Particle Data Group), Phys. Rev. D 110, 030001 (2024)
- [30] M. Gronau, O. F. Hernandez, D. London *et al.*, Phys. Rev. D 52, 6356 (1995)
- [31] D. Xu, G. N. Li, and X. G. He, Int. J. Mod. Phys. A 29, 1450011 (2014)
- [32] X. G. He, G. N. Li, and D. Xu, Phys. Rev. D **91**, 014029 (2015)
- [33] M. Gronau, O. F. Hernandez, D. London *et al.*, Phys. Rev. D 50, 4529 (1994)
- [34] D. Wang, C. P. Jia, and F. S. Yu, JHEP **21**, 126 (2020)

- [35] M. Ablikim *et al.* (BESIII), Phys. Rev. D **96**, 112006 (2017)
- [36] B. Zheng *et al.* (BESIII), PoS **Hadron2017**, 096 (2018)
- [37] M. Ablikim *et al.* (BESIII), arXiv: 2502.08929 [hep-ex]
- [38] R. Aaij et al. (LHCb), Phys. Rev. D 108, 032010 (2023)
- [39] M. Ablikim *et al.* (BES), Phys. Rev. D **74**, 072001 (2006)
- [40] M. Ablikim *et al.* (BESIII), Chin. Phys. C **44**, 040001 (2020)
- [41] M. N. Achasov et al., Phys. Usp. 67, 55 (2024)
- [42] A. E. Bondar *et al.* (Charm-Tau Factory), Phys. Atom. Nucl. **76**, 1072 (2013)
- [43] H. P. Peng, Y. H. Zheng, and X. R. Zhou, Physics 49, 513 (2020)
- [44] M. Ablikim *et al.* (BESIII), Chin. Phys. C **48**, 123001 (2024)